An alternative splicing modulator decreases mutant HTT and improves the molecular fingerprint in Huntington's disease patient neurons

Florian Krach
University of Erlangen-Nuremberg https://orcid.org/0000-0002-4506-8792
Judith Stemick
University of Erlangen-Nuremberg https://orcid.org/0000-0002-0750-6130
Tom Boerstler
University of Erlangen-Nuremberg https://orcid.org/0000-0001-9920-9012
Alexander Weiss
Evotec SE
Ioannis Lingos
Evotec SE
Holger Meixner
University of Erlangen-Nuremberg
Sonja Plötz
University of Erlangen-Nuremberg
Michaela Farrell
University of Erlangen-Nuremberg
Ute Hehr
Center for Human Genetics Regensburg
Zacharias Kohl
University Hospital Regensburg
Beate Winner
FAU Erlangen-Nuernberg https://orcid.org/0000-0002-6909-0564
Jürgen Winkler (Juergen.Winkler@uk-erlangen.de)
University of Erlangen-Nuremberg https://orcid.org/0000-0003-0630-9204

Article

Keywords:

Posted Date: May 3rd, 2022

DOI: https://doi.org/10.21203/rs.3.rs-1551505/v1

Version of Record: A version of this preprint was published at Nature Communications on November 10th, 2022. See the published version at https://doi.org/10.1038/s41467-022-34419-x.

Abstract

Huntington's disease (HD) is a neurodegenerative disorder caused by poly-Q expansion in the Huntingtin (HTT) protein. Here, we delineate elevated mutant HTT (mHTT) levels in patient-derived cells including fibroblasts and iPSC derived cortical neurons using a GLP approved HTT assay. HD patients' fibroblasts and cortical neurons recapitulate aberrant alternative splicing as a molecular fingerprint of HD. Branaplam is a splicing modulator currently tested in a phase II study in HD (NCT05111249). The drug lowers total HTT (tHTT) and mHTT levels in fibroblasts, iPSC, cortical progenitors, and neurons in a dose dependent manner at an IC_{50} consistently below 10nm without inducing cellular toxicity. Branaplam promotes inclusion of non-annotated novel exons. Amongst, a 115bp frameshift-inducing exon in the HTT transcript in Branaplam treated cells from Ctrl and HD patients leading to a profound reduction of HTT RNA and protein levels. Importantly, Branaplam ameliorates aberrant alternative splicing in HD patients' fibroblasts and cortical neurons. These findings highlight the applicability of splicing modulators in the treatment of CAG repeat disorders and decipher their molecular effects associated with the pharmacokinetic and -dynamic properties in patient-derived cellular models.

Introduction

Huntington's disease (HD) is a progressive neurodegenerative disorder caused by CAG-repeat expansion in the coding region of the HTT transcript, leading to an elongated polyglutamine (poly-Q) stretch in HTT [1]. While individuals with 39 and above CAG-repeats in one allele will develop HD, a repeat length below 36 is non-pathogenic. Intermediate repeat lengths in the range between 36 and 39 may cause HD with incomplete penetrance [2]. The elongated poly-Q, mutant HTT (mHTT) is suspected to exhibit a toxic gain of function resulting in neuronal toxicity [3].

Clinically, HD is characterized by the triad of motor dysfunction, psychiatric symptoms, and cognitive deficits. Motor symptoms, most prominently chorea, are related to the degeneration of striatal medium spiny neurons [2] and subsequently cortical projection neurons. Interestingly, cortico-striatal projections are affected years prior disease onset. [4]. Specifically, degeneration of pyramidal neurons in the primary motor cortex and anterior cingulate cortex lead to more pronounced motor and mood impairments, respectively [5,6] .

So far, there is no causal therapy to improve or even halt the disease course of HD. However, a number of recent clinical trials focus on small compounds lowering HTT levels [7]. One of the latest clinical trials investigates the effectiveness of the alternative splicing (AS) modulator Branaplam (previously called LMI070, NVS-SM1) in HD (NCT05111249). Branaplam was initially designed for spinal muscular atrophy (SMA) and promotes inclusion of exon 7 in the SMN2 transcript via stabilization of the pre-mRNA - U1 snRNP complex [8].

Here, we describe Branaplam's mechanism of action and effects in HD. We develop a HD patient-derived cellular platform to investigate mHTT levels using a validated HTT assay. We demonstrate that

Branaplam is able to reduce mHTT levels and restore aberrant splicing, an important molecular feature in HD. We evaluate the precise pharmacokinetic and -dynamic properties of Branaplam in primary fibroblasts and iPSC-derived cortical neurons of controls and HD patients. Lastly, we explore the small molecule 's potential to revert molecular phenotypes of HD patients' neurons.

Results

mHTT is increased in cellular model of HD patients

We chose to use various patient-derived non-neuronal and neuronal cells to model HD in vitro (Fig. 1A). Besides 4 Ctrls, we recruited 4 HD patients originating from 3 distinct families (Table 1 and Extended Data Fig. 1A). The CAG repeats on the affected allele ranged from 39–57 (Table 1). Clinically, all patients presented motor symptoms. Hence, we reprogrammed fibroblasts into iPSC and subsequently differentiated them into cortical neurons using a previously published dual-SMAD-inhibition based protocol [9]. At day 25 of differentiation, $NESTIN^{+}/PAX6^{+}$ cortical progenitors were observed (Fig. 1B and Extended Data Fig. 1B-C) and from day 35 on deep layer cortical neurons positive for CTIP2 were apparent (Fig. 1C-D and Extended Data Fig. 1D-E). No differences in differentiation capabilities between Ctrl and HD were detected (Fig. 1B and C).

Table 1
HD and Ctrl cohort. HD: Huntington's disease, Ctrl: Control. * marks iPSC line setup used for all experiments starting Fig. 2. Underlined parts of IDs indicate abbreviated form of line name used in figures.

donor	gender	Age at biopsy	CAG repeats	fibroblast ID	iPSC ID
HD	f	44	16 / 40	UKERf4Q4	UKERi4Q4-S1-105
					UKERi4Q4-S1-109*
HD	m	54	15 / 39	UKERfOP5	UKERiOP5-S1-106*
					UKERiOP5-S1-108
HD	m	26	18 / 50	UKERf59H	UKERi59H-S1-101
					UKERi59H-S1-103*
					UKERi59H-S1-108
HD	f	23	28 / 57	UKERf919	UKERi919-S1-101*
Ctrl	f	45	15 / 16	UKERf33Q	UKERi33Q-S1-109*
Ctrl	m	43	17 / 21	UKERfB26	UKERiB26-S1-007
					UKERiB26-S1-018*
Ctrl	m	52	18 / 19	UKERf4CC	UKERi4CC-S1-007
					UKERi4CC-S1-015*
Ctrl	m	32	16 / 17	UKERf4L6	UKERi4L6-S1-027*
					UKERi4L6-S1-032

Next, we determined the total (tHTT) and mHTT levels in cellular homogenates. We used a clinical grade immune absorbent-based, meso scale discovery (MSD) assay with an electro-chemiluminescent readout. This assay allows the molar quantification of tHTT and mHTT levels by comparing to a standard of recombinant HTT with 23 and 73 glutamines, respectively (Fig. 1E) [10]. While tHTT levels were unchanged in all cell types analyzed, a substantial increase in mHTT levels was observed in HD-patient iPSC, cortical progenitors, and cortical neurons (Fig. 1F-I). Hence, our cellular platform is suitable to detect changes in mHTT levels in non-neuronal and neuronal cells.

HD patient-derived cells exhibit aberrant RNA missplicing as a molecular disease phenotype

Aberrant AS events are present in patients' primary motor cortex [11] and striatum [12]. Therefore, we investigated whether HD-patients' cells also exhibit this molecular fingerprint by performing deep long read RNA-sequencing of HD and Ctrl fibroblasts (4 patients vs. 4 healthy controls) and iPSC-derived cortical neurons (3 patients vs. 3 healthy controls) (Figure 2A). We identified 306 and 1,437 significantly

(FDR <0.05; inclusion level difference > 0.1) differentially spliced exons (SE) in fibroblasts (Figure 2B) and iPSC-derived cortical neurons of HD patients (Figure 2C), respectively, consisting mostly of cassette exons (Figure 2D and E). Eleven included and excluded events were shared between HD fibroblasts and HD cortical neurons (Figure 2F). Next, we asked which upstream alternative splicing factors may regulate these changes. Therefore, we made use of the ENCODE enhanced cross-linking and immunoprecipitation (eCLIP) sequencing experiments, providing RNA-binding profiles of a large number of RNA-binding proteins (RBPs) [13]. We investigated whether binding of these proteins to the RNA of HD AS sites encompassing the region from the upstream exon start site to the downstream exon end was enriched over background. HD-AS events in fibroblasts and iPSC-cortical neurons were enriched for distinct RBPs (Figure 2G and H). Interestingly, HD-AS events in iPSC-cortical neurons were enriched for binding sites of RBFOX2, TIA1, and U2AF2 (Figure 2H). Importantly, identical RBPs were previously implicated in aberrant AS in HD *postmortem* tissue [12]. This suggests that aberrant RNA missplicing is present in HD patients' fibroblasts and to a larger extent in iPSC derived cortical neurons. In conclusion, HD patients' iPSC cortical neurons recapitulate aberrant AS as a major molecular pattern of HD.

Branaplam/LMI070 reduces total and mutant HTT protein levels in HD patients' cells

Therapeutic strategies in HD aim at lowering HTT levels to reduce mHTT toxicity. A recently initiated phase II study repurposes the small molecule AS modulator Branaplam (LMI070, NCT05111249). Hence, we sought to investigate its effects to specifically reduce mHTT levels and its impact on Ctrl and HD-derived cells (Figure 3A). Branaplam exhibited dose-dependent effects in lowering HTT levels in fibroblasts and iPSC (Figure 3B and C, tHTT). Similar trends were visible for mutant HTT in HD patients' cells (Figure 3B and C, mHTT). Interestingly, Branaplam treatment did not induce cellular toxicity in fibroblasts and iPSC (Figure 3B and C, toxicity). In order to investigate the pharmacokinetic properties of Branaplam *in vitro*, we performed a dose-response experiment in cortical progenitor cells. The half-maximal inhibitory concentration (IC_{50}) of Branaplam was consistently below 10nM, reducing total as well as mHTT levels without affecting cellular toxicity (Figure 3D). A concentration of 10nM reduced tHTT levels in iPSC-derived cortical neurons by 38.8% and mHTT levels in HD patients by 21.8% without inducing toxicity (Figure 3E). To explore potential toxic effects of Branaplam on neuronal subtypes, we investigated Caspase 3/7 activation in deep layer CTIP2-positive neurons. Branaplam did not induce cell death in CTIP2+ and CTIP2- neurons (Figure 3F and Extended Data Figure 2). In summary, these findings suggest that Branaplam efficiently reduces total and mutant HTT protein levels in various Ctrl and HD patient-derived cell types without inducing toxicity.

Branaplam promotes inclusion of previously non-annotated novel splice sites

Next, we explored how the splicing modulator Branaplam results in reduced HTT protein levels. We performed a streamlined alternative splicing analysis in fibroblasts and cortical neurons of controls and HD patients with and without Branaplam treatment to decipher Branaplam's targets, sequence preferences, and effects on gene expression in an unsupervised manner (Figure 4A). Significantly differentially spliced events upon Branaplam treatment in all four cohorts (Ctrl fibroblasts, HD fibroblasts,

Ctrl cortical neurons, HD cortical neurons) were grouped using k-means, resulting in 10 distinct clusters (cluster 0 - cluster 9) (Figure 4B). Cluster 6 and cluster 9 exhibited coherent, unidirectional alternative splicing changes (exon inclusion) in all four cohorts (Figure 4C and D, Extended Data Figure 3A). Interestingly, more than 50% of events in both clusters were novel splice sites (novelSS) that represent previously non-annotated exons (Figure 4C and D, pie charts). In contrast to the annotated exons, the 55 novelSS exons are vastly excluded in untreated cells and only become apparent after Branaplam treatment (Figure 4E and Extended Data Figure 3B). Next, we analyzed if those novel, Branaplam-dependent exons exhibited enrichment of specific sequences around their 5' and 3' splice site by analyzing 4mer, 6mer and 8mer sequences (Figure 4F and G). Interestingly, even at the 8mer level we identify enriched sequences at the 3' splice site (TTCAGTTT) and 5' splice site (AGAGTAAG) (Figure 4G) suggesting, at least in part, a sequence-dependent mode of action of Branaplam. NovelSS exons may contain STOP codons or result in an out-of-frame transcript potentially leading to nonsense mediated RNA decay and mRNA degradation. Therefore, we analyzed gene expression changes of the transcripts that contain the 55 newly identified Branaplam-induced exons. Three transcripts (DLGAP4, LARP7 and KDM6A) exhibited a consistent increase in gene expression (Figure 4H). Interestingly, we identified that the levels of FHOD3, PAPD4 and also HTT were consistently reduced in all four comparisons (Figure 4H).

We further evaluated the HTT transcript and detected an inclusion of a 115b long frameshift-inducing exon with 2 STOP codons between exon 49 and exon 50 upon Branaplam treatment (Figure 5A - C). This splice site contained the previously identified Branaplam associated 5' splice site sequence AGAGTAAG (Figure 5A). We further validated the integration of this exon by RT-PCR with primers annealing to the flanking exons (Figure 5A, blue arrows). A consistent integration of this exon in all analyzed Ctrl and HD patient fibroblasts and cortical neurons was observed (Figure 5D - G), leading to reduced HTT mRNA levels (Figure 5H and I). In summary, these findings suggest that Branaplam promotes novelSS exon inclusion with distinct sequence preferences. This is present in HTT transcripts leading to a nonsense mediated RNA decay isoform and a profound reduction of HTT levels.

Aberrant alternative splicing pathology in HD is ameliorated by Branaplam

We have identified aberrant AS in HD fibroblasts and iPSC derived cortical neurons as a molecular HD fingerprint (Figure 2). We next investigated if Branaplam treatment, and the accompanied reduction in mutant HTT levels, improves this AS deficiency in HD (Figure 6A). Branaplam significantly reduced the absolute inclusion level differences of HD AS events by 27.6% in fibroblasts and 28.6% in iPSC derived cortical neurons (Figure 6B and C). 53.2% of HD AS events in fibroblasts (Figure 6D-F) and 47.9% of HD AS events in iPSC derived cortical neurons (Figure 6G-I) exhibited an absolute inclusion level difference below our threshold of 0.1 upon Branaplam treatment. This suggests that Branaplam reverts HD AS events, ameliorating a prominent molecular signature in HD.

Discussion

This study describes the reduction of mutant HTT levels in HD patients' fibroblasts and iPSC derived cortical neurons by application of the splicing modulator Branaplam without inducing cellular toxicity. Specifically, we show that aberrant AS is ameliorated following Branaplam treatment.

Various approaches that were and still are under clinical development for the treatment of HD focus on lowering HTT levels. This includes antisense oligonucleotides (ASOs)[14] (Generation HD 1: NCT03761849; Precision HD-1: NCT03225833; Precision HD-2: NCT03225846) and adeno-associated virus (AAV)-mediated gene therapeutic delivery of RNAi-based machineries (NCT04120493), currently both on hold. Both approaches are dependent on repeated intrathecal or stereotactic injections. In contrast, Branaplam is an orally available small molecule, much easier applicable in HD patients.

Here, we delineated the mechanism of action of Branaplam in two distinct cell types in Ctrl and HD patients. Branaplam was originally designed to promote inclusion of exon 7 in the SMN2 transcript as an intervention for SMA[8]. We reveal that Branaplam also induces inclusion of multiple non-annotated novel exons, preferentially exons with AGAGTAAG sequences at their 5' splice site. Amongst, a frameshift-inducing exon is included in the HTT transcript, leading to a profound lowering of tHTT and mHTT levels in Ctrl and HD patient cells. A recent study identifies a similar mechanism of action of Branaplam in a permanent neuroblastoma cell line of human origin [15]. Furthermore, we confirmed the mechanism of action in multiple Ctrl and HD patient cell types, including iPSC-derived cortical neurons. Additionally, we precisely defined the pharmacokinetic properties of the small molecule AS modifier using validated quantitative assays for of tHTT and mHTT that showed an IC_{50} consistently below 10nM in Ctrl and HD patient cells. We further underscore the effectiveness of this molecule by providing compelling evidence that Branaplam ameliorates a molecular fingerprint in HD. On a broader scope, we emphasize the applicability of AS modulators to alter pathological protein levels by integration of non-annotated exons and restore molecular fingerprints using primary fibroblasts of HD patients and patient iPSC-derived cortical neurons.

Methods

Subjects and human samples

The generation and use of human iPSCs was approved by the Institutional Review Board (Nr. 4120: *Generierung von humanen neuronalen Modellen bei neurodegenerativen Erkrankungen*). Formal informed consent was obtained from all subjects. Four patients from three different families and age matched controls without history of neurological disorders were recruited. CAG repeats of fibroblasts and iPSCs were measured by the center of Human Genetics at the University Hospital Regensburg (Ute Hehr, MD).

Fibroblast culture

Fibroblasts were resuspended in fibroblast growth medium (FGM, 75% DMEM, 15% FCS, 2mM L-Glutamine, 100µg/ml Penicillin/Streptomycin, 2ng/ml fibroblast growth factor 2) and plated on polystyrene cell culture flasks. Medium was changed twice a week. Fibroblasts were split by removing

FGM, adding Trypsin supplemented with 0.05% ethylenediaminetetraacetic acid (EDTA) and incubating at 37°C until cells detach. FGM was added to the detached cells, the cell suspension was transferred to a centrifugation tube and processed for 5 minutes at 300g RT. Supernatant was removed, cells were resuspended in FGM and plated on a new polystyrene cell culture flask.

iPSC generation and culture

For iPSC generation, skin biopsies of study participants were obtained. iPSCs were generated from fibroblasts using the CytoTune iPS 2.0 Sendai Reprogramming Kit (Thermo Fisher Scientific) according to the manufacturer's instructions. Therefore, cell lines were transduced with Sendai virus containing four reprogramming factors c-MYC, KLF4, OCT3/4, and SOX2.

After generation, iPSCs were cultured in human stem cell media StemMACS iPS-Brew XF (Miltenyi Biotec) supplemented with 100 U/mL penicillin/streptomycin on 4mg/ml Geltrex (Gibco^{TM}) coated polystyrene cell culture plates. Medium was changed every other day. When cell cultures reached 70-80% confluency, cells were passaged. Afterwards, iPSCs were washed once with DMEM/F12 (Gibco^{TM}) and incubated with Gentle Cell Dissociation Reagent (Stemcell technologies) for 5 minutes at room temperature (RT). Gentle Cell Dissociation Reagent was aspirated and StemMACS iPS-Brew XF supplemented with 100 U/mL penicillin/streptomycin was added. Corning® Cell Lifter was used to detach hiPSCs from the cell culture plate. iPSCs were transferred to a new Geltrex coated plate.

Cortical differentiation

iPSCs were differentiated into cortical neurons using a previously reported protocol [9]. In brief, iPSCs were maintained as described above. iPSCs were dissociated into a single cell suspension upon 70-80% confluency. Cells were washed once with PBS w/o Mg2+/Ca2+ and were incubated with Accutase for 5 min at 37°C. Cells were washed with DMEM/F12, centrifuged for 3 min at 300 g at RT, and resuspended in StemMACS iPS-Brew XF supplemented with 10 µM ROCK inhibitor. Cells were seeded on Geltrex coated plates with the desired density of 300'000 cells per cm^2 and incubated for 24h at 37°C, 5% CO2. After cells reached confluency the next day, the medium was changed to neural maintenance medium (NMM: DMEM/F-12, neurobasal/B-27/N2, 100µM GlutaMAX, 100µM non-essential amino acids, 50 µM 2-mercaptoethanol, 1x penicillin-streptomycin) supplemented with dual SMAD inhibitors (NIM: 10µM SB431542, 100nM LDN193189) to promote neural induction. On day 12, cells differentiated into a neuroepithelial sheet and were further passaged. Cell sheet was gently washed with DMEM/F-12 and incubated for 5min with Collagenase V (2mg/ml) at 37°C for 5 min. The cell sheet was gently washed twice with DMEM/F-12 and finally detached with a 5ml serological pipette in NIM and gently resuspended into smaller pieces. Cells were passaged in a 1:2 ratio on Geltrex coated plates. Medium was changed to NMM the next day. Upon appearance of neural rosettes, medium was changed for 2 days in NMM supplemented with 20ng/ml FGF2 to promote neural stem cell proliferation. On day 19, cells were further passaged and maintained in NMM with medium changes every second day. On day 30, cells were finallly single-cell passaged with Accutase with the desired density of 50'000 cells per cm^2. Cells were

maintained in NMM for neuronal differentiation with medium changes twice a week till day 35 (Figure 1) or day 50 (Figures 2 – 6).

Branaplam treatment

Branaplam was reconstituted in DMSO with a concentration of 5M. Branaplam was supplemented to the cell culture media (FGM, StemMACS iPS-Brew XF or NMM) with a final concentration of 0.46nM - 1000nM and 0.002% DMSO. Supplemented medium was changed every 24h for a total of 72h.

Immunofluorescent staining

Cells were fixed in 4% paraformaldehyde (PFA) for 20 mins at RT and subsequently washed 3x with PBS each. The cells were permeabilized using 0.1% Triton X-100 and in PBS for 20 mins at RT. Then, cells were blocked in 0.3% Triton-X100 and 3% donkey serum in PBS for 1h at RT. Afterwards, cells were incubated with primary antibodies (rat anti CTIP2: ab18465, Abcam, 1:500; mouse anti beta-III-Tubulin: G7121, Promega, 1:1000; rabbit anti PAX6, 901301, BioLegend, 1:200; mouse anti Nestin, MAB5326, Millipore, 1:500) at 4°C overnight. After washing, incubation with secondary antibodies and nuclei staining using 1µg/ml DAPI was performed. The slides were mounted using ProLong(r) Antifade (Invitrogen) solution. Imaging was performed with a Zeiss Laser scanning 780 inverted confocal microscope.

FACS analysis

For flow cytometry, cells were dissociated using Accutase for 30 mins at 37°C and resuspended in FC buffer (2% FCS, 0.01% sodium azide in PBS). Cells were dispensed into 5 ml tubes (Sarstedt) at 500,000 cells per well. For intracellular antigens, cells were fixed and permeabilized using 100ul BD Fixation/Permeabilization Solution (BD Bioscience) for 10 mins, then 1ml of BD Perm/Wash Buffer was added, cells were incubated for 5 mins and subsequently centrifuged at 1,500 rpm for 3 mins. For intracellular staining of cortical progenitors anti-PAX6-APC (130-123-267, Miltenyi Biotech, 1:100) and anti-NESTIN-PerCp-Cy5.5 (561231, BD Bioscience, 1:100) for an additional 30 mins. After a wash step, cells were resuspended in 350µl FACS buffer containing DAPI (1µg/ml). For intracellular staining of neurons, cells were stained using anti-bIII-Tubulin-AF405 (NB600-1018AF405, NovusBio, 1:100) or anti-CTIP2-FITC (ab123449, Abcam, 1:100) for 30 mins. Additional controls included applying an antibody solution without one antibody in the full cocktail (“minus 1 control”) and were used to determine potential bleed-through of the fluorophores. The flow cytometry experiments were performed with a Cytoflex S machine (laser 405nm, 488nm, 561nm and 638nm; Beckman Coulter) and analyzed with the CytExpert 2.4 software.

To determine cell death via FACS, we used a commercially available kit that uses a fluorescent 660-DEVD-FMK caspase-3/7 inhibitor reagent (ab270785, abcam) and a fixable cell permeability dye (Live-or-Dye, 32008-T, Biotium). The caspase assay and Live-or-Dye assay reagents were dissolved in 50ul DMSO, respectively and aliquoted and stored at -20°C. For the assay, cortical neurons were grown in 24-well plates. At the day of analysis, media was aspirated from the plate and 150µl DMEM/F12+Glutamax

containing 0.48µl 660-DEVD-FMK caspase-3/7 inhibitor reagent and 0.15µl Live-or-Dye assay were applied. After incubation for 45 mins at 37°C. Cells were dissociated, fixed, and stained as stated above. To precisely assess bleed through, single incubation controls (either with 660-DEVD-FMK caspase-3/7 inhibitor reagent or Live-or-Dye assay) were used. The number of Casp3/7+Live-or-Dye- cells vs. Casp3/7-Live-or-Dye- were determined in CTIP2+ and betaIII-Tubulin+ cells.

Protein extraction

Lysis buffer (150 mM NaCl, 20 mM Tris-HCl (pH 7.5), 1 mM EDTA, 1 mM EGTA, 1 % Triton-X-100, 10 mM NaF, 1 mM PMSF, 1x Phosphatase Inhibitor, and 1x Protease Inhibitor in dH_2O) was added to the cells for 30 mins at 4°C. Cell lysate was transferred into a tube and centrifuged for 15 mins at 2000g at 4°C. Supernatant was transferred to a new centrifugation tube and stored at -80°C. Protein concentration was determined using BCA assay kit (Thermo Fisher Scientific) measuring with CLARIOStar Plus (BMG Labtech).

HTT assay

Meso-Scale-Discovery (MSD) assays to measure total and mutant Huntingtin protein levels were performed by Evotec SE, Hamburg [10]. The MSD assay plate was coated with 5ug/ml of the N-terminally binding HTT antibody 2B7 (#CH03023, Coriell) in coating buffer (15mM Na2CO3, 35mM NaHCO3) overnight. The next day, the plate was washed 3x in wash buffer (0.2% (v/v) Tween 20 in DBPS), blocked for 1h at RT shaking at 350rpm (2% (w/v) Probumin in wash buffer) and subsequently washed 3x again. The MSD plate was then incubated with the protein sample derived from the various cells (10ul sample/well) for 1h at RT shaking at 350rpm. In parallel, a standard of defined concentrations of recombinant human HTT with 23Q or 73Q was applied. After incubation, the plate was washed 3x in wash buffer. Next, 10ul of the detection antibodies were added to the MSD plates: 0.5ug/ml D7F7 antibody (#5656, Cell Signaling) for tHTT detection, or 5ug/ml MW1 antibody (#MABN2427, Sigma-Aldrich) binding the polyQ region in exon 1 for mutant HTT detection. MW1 was used directly labeled with a SULFO-Tag and incubated for 1h at RT shaking at 350rpm and subsequently washed 3x. For D7F7, after 3 washes, a SULFO-Tag-labelled anti-rabbit secondary antibody (MSD) was incubated for 1h at RT and the plate subsequently washed 3x. MSD read buffer was added to the plate. If the detection antibody binds to the sample in close proximity to the MSD plate an electrochemiluminescent signal is emitted and detected at 620nm. The total and mutant HTT levels were calculated according to the generated standard curves and normalized to protein input.

Toxi light assay

Cytotoxicity was measured during Branaplam treatment using the ToxiLight Bio assay kit (Lonza) according to the manufacturer's instructions. Therefore, supernatant was collected after 72h of Branaplam treatment. The positive control was supernatant of untreated cells incubated with 10% Triton-X100 for 20 minutes at 37°C. Triplicates 20µl/sample were transferred to a 96-Well. 100µl of adenylate

kinase detection reagent (ToxiLight Bio assay kit, Lonza) was added and incubated for 5 mins at RT. The resulting luminescence was measured by the CLARIOStar Plus (BMG Labtech).

RNA extraction and HTT novel exon PCR

RNA was extracted using the RNeasy kit (Qiagen) according to the manufacturer's instructions. RNA concentrations were measured using a NanoDrop. The GoScript Reverse Transcriptase cDNA Synthesis kit (Promega) was used to generate cDNA from fibroblasts and cortical neurons using random primers. RNA was mixed with random primers and incubated for 5 mins at 70°C and placed on ice for 5 mins. The remaining reaction mix was added and incubated for 5 mins at 25°C, followed by 1h 42°C extension period and a 15 mins 70°C inactivation. The GoTaq 2x Mastermix (Promega) was used to amplify novel exon inclusion in HTT amplifying 0.5ul of template with 1ul of fwd primer (100uM stock, GTCATTTGCACCTTCCTCCT) and 1ul rev primer (100uM stock, TGGATCAAATGCCAGGACAG), 5ul Mastermix and 2.5ul DNase/RNase-free water. Primer sequences were obtained from the Novartis patent (WO2021084495A1). The mix was amplified with the following conditions: 95°C for 3min, and 34 cycles of 95°C for 30s, 60°C for 20s and 72°C for 60s. A final extension of 72°C for 5min was added at the end. The products were run on a 2% Agarose gel with RotiGel stain. (Carl Roth GmbH) at 125V. A random selection of 88bp and ~200bp bands in Ctrl and HD was cut out and purified to verify their correct identity by Sanger sequencing.

RNA sequencing

A total of 500ng per sample were sent for RNA sequencing to Azenta Life Sciences (Genewiz Leipzig, Germany) for 150bp paired-end sequencing with Poly-A selection. For fibroblasts 4 Ctrl samples and 4 HD samples with DMSO or Branaplam treatment were sent and sequenced at a depth of >20 million reads in each sample. For iPSC-derived cortical neurons, 3 Ctrl samples and 3 HD samples with DMSO or Branaplam treatment were sent and sequenced at a depth of >37 million reads in each sample. After obtaining the fastq files, adapters were trimmed using Trimmomatic [16] and aligned to the human genome (GRCh38) using STAR [17]. In every sample >90% of reads mapped uniquely to the human genome. Reads were assigned to genes in the gencode annotation (version 26) using the featureCounts module within the Subread package [18]. Reads Per Kilobase of transcript, per Million mapped reads (RPKM) were calculated from the obtained counts to normalize for gene expression.

Alternative splicing analysis

For differential splicing rMATS (version 4.2.0) [19] was used with the –novelSS flag to identify non-annotated exons. The gencode annotation (version 26) was used to define known exons. The output files considering only the junction counts were used for further analysis. A negative value of the InclusionLevelDifference reflects an inclusion of a given exon in the samples of the target condition and a positive value of the InclusionLevelDifference reflects an exclusion of a given exon in the samples of the target condition. Subsequently, the files from the different splice types (cassette exon, A5SS, A3SS, RI and MXE) were combined into one file.

All downstream analysis were performed in Python 3. Only exon junctions that were covered with at least 10 counts in each sample of a given dataset were considered. A unique index was generated, referring to a specific AS event with the aim to identify the identical exon junction in separate rMATS analysis. An exon was called as differentially alternatively spliced in each dataset if the FDR was below 0.05 and the absolute value of the InclusionLevelDifference was more than 0.1. The overlap of differentially spliced events was visualized with the Venn function in matplotlib library.

For k-means clustering, the k-means method from the sklearn.cluster module from sciki-lean was used (specifications: init='ranodm', n_clusters=10, n_init=10, max_iter=300, random_state=42). AS events significant in any of the four comparisons (fibroblasts-Ctrl DMSO vs Branaplam, fibroblasts-HD DMSO vs Branaplam, cortical neurons-Ctrl DMSO vs Branaplam, cortical neurons-HD DMSO vs Branaplam) datasets were clustered into 10 clusters according to the inclusion value differences in the respective dataset. Exon junctions that were not detected with a sufficient number of reads were masked and visualized in black. The inclusion level difference of each cluster was additionally visualized with violin plots.

To determine the effect of aberrant AS reversal upon Branaplam treatment, the individual inclusion values were used from HD-DMSO, HD-Branaplam, and Ctrl-DMSO samples in fibroblasts and cortical neurons, respectively. Only significant HD alternative splicing events (Ctrl DMSO vs. HD DMSO) in a respective cell type that were detected in all samples analyzed in a cell type (>10 reads in every single sample) were used. The reversal of aberrant AS was investigated in a quantitative and qualitative manner. For quantitative measurement, the absolute inclusion value difference was calculated by subtracting HD-DMSO or HD-Branaplam inclusion values from Ctrl-DMSO inclusion values and taking the absolute value. The statistical significance of the absolute inclusion level difference was determined using scipy.stats.ranksums. For qualitative measurement, the mean inclusion values of Ctrl-DMSO and HD-DMSO and HD-Branaplam samples in each cell type were also visualized in a scatter plot. A reversal of aberrant AS was determined if the inclusion level differences in HD-Branaplam samples dropped below an absolute value of 0.1.

RBP enrichment

In order to determine RNA-binding proteins that are enriched in alternatively spliced events in HD, we made use of the ENCODE database and their eCLIP-seq datasets. We downloaded eCLIP seq peak files aligned to GRCh38 with the Irreproducible Discovery Rate (IDR) peaks (released by November 2021). A peak was considered significant if negative $\log_{10}$(P value) ≥ 3 and the $\log_2$(fold change) ≥ 3. To determine if an eCLIP-seq peak was present in an exon junction in HD, the rMATS output (fibroblasts Ctrl-DMSO vs HD-DMSO or cortical neurons Ctrl-DMSO vs HD-DMSO) of interest was converted into a bed format encompassing the region starting from the upstream exon start to the downstream exon end. The rMATS bed was intersected with the significant eCLIP-seq peak file using pybedtools (-u True). The statistical significance of the enrichment was computed using hypergeometric test with all events that passed the coverage threshold as the background.

Kmer enrichment

To determine the sequence preferences of Branaplam-induced AS sites at the 3' and 5' splice site, we calculated kmer enrichments (4mer, 6mer, and 8mer) 5b upstream and downstream of the 3' and 5' splice site, respectively. As a background, we also calculated the 5b upstream and downstream of the 3’ splice site of the respective upstream exon and the 5' splice site of the respective downstream exon. Kmers were counted with Kvector (https://github.com/olgabot/kvector) and significance was determined with Fisher's exact test using scipy.stats.

Statistical analysis

GraphPad Prism 9 was used to visualize data and calculate statistics for pair-wise and grouped analyses (HTT protein measurements, toxilight assay, FACS quantification, densitometric quantification of HTT PCR, HTT RPKM values). DMSO samples and their respective Branaplam samples were considered as paired. Normal distribution was assessed with Shapiro-Wilk test. When comparing two conditions, Welch's test was used if normal distribution was confirmed and Mann-Whitney test was used for non-normally distributed data. When comparing multiple groups (e.g. different Branaplam concentrations), one-way ANOVA with Geisser-Greenhouse correction was used if normal distribution was confirmed and Friedman test was used for non-normally distributed data with Dunnett's or Dunn's post hoc test respectively to identify differences between individual groups. For grouped analyses (e.g. DMSO vs. Branaplam in Ctrl vs. HD), two-way ANOVA was used. The statistical test used for calculating significance of each graph is indicated in the figure legend. A p value ≤ 0.05 was considered as significant.

Declarations

Data availability

All intermediate files (e.g. rMATS outputs, counts, quantifications) are submitted within the extended data. Due to the European General Data Protection Regulation and specifically patient consent of study participants who donated biological material used for the generation of the RNA-seq datasets, access will be granted from the corresponding authors upon reasonable request. Furthermore, any additional data and information may be acquired from the corresponding author upon reasonable request.

Acknowledgements

We would like to thank all patients and control individuals who donated biological material to conduct this study. We thank Naime Denguir, M.Sc. and Dr. Wolfgang Krebs (CUBIDA core unit) for technical support. JS is a graduate student of the research training group 2162 “Neurodevelopment and Vulnerability of the Central Nervous System” of the Deutsche Forschungsgemeinschaft (DFG 270949263/GRK2162 (BW, JW)). FK was supported by the Interdisciplinary Center for Clinical Research (IZKF) at the University Hospital Erlangen (Junior Project [J88]). Additional support came from the Bavarian Ministry of Science and the Arts in the framework of the ForInter network (BW, JW), the

TreatHSP consortium (BMBF 01GM1905B to BW, JW), the German Research Foundation, DFG WI 3567/2-1 (BW) and and the IZKF advanced project E30 (BW, JW).

Conflict of interest

All other authors do not have competing conflicts of interest regarding this study.

References

1. A novel gene containing a trinucleotide repeat that is expanded and unstable on Huntington's disease chromosomes. The Huntington's Disease Collaborative Research Group. Cell **72**, 971–983, doi:10.1016/0092-8674(93)90585-e (1993).
2. Ross, C. A. *et al.* Huntington disease: natural history, biomarkers and prospects for therapeutics. Nat Rev Neurol **10**, 204–216, doi:10.1038/nrneurol.2014.24 (2014).
3. Jimenez-Sanchez, M., Licitra, F., Underwood, B. R. & Rubinsztein, D. C. Huntington's Disease: Mechanisms of Pathogenesis and Therapeutic Strategies. Cold Spring Harb Perspect Med **7**, doi:10.1101/cshperspect.a024240 (2017).
4. Rosas, H. D. *et al.* Cerebral cortex and the clinical expression of Huntington's disease: complexity and heterogeneity. Brain **131**, 1057–1068, doi:10.1093/brain/awn025 (2008).
5. Macdonald, V. & Halliday, G. Pyramidal cell loss in motor cortices in Huntington's disease. Neurobiol Dis **10**, 378–386, doi:10.1006/nbdi.2002.0528 (2002).
6. Thu, D. C. *et al.* Cell loss in the motor and cingulate cortex correlates with symptomatology in Huntington's disease. Brain **133**, 1094–1110, doi:10.1093/brain/awq047 (2010).
7. Marxreiter, F., Stemick, J. & Kohl, Z. Huntingtin Lowering Strategies. Int J Mol Sci **21**, doi:10.3390/ijms21062146 (2020).
8. Palacino, J. *et al.* SMN2 splice modulators enhance U1-pre-mRNA association and rescue SMA mice. Nat Chem Biol **11**, 511–517, doi:10.1038/nchembio.1837 (2015).
9. Shi, Y., Kirwan, P. & Livesey, F. J. Directed differentiation of human pluripotent stem cells to cerebral cortex neurons and neural networks. Nat Protoc **7**, 1836–1846, doi:10.1038/nprot.2012.116 (2012).
10. Reindl, W. *et al.* Meso scale discovery-based assays for the detection of aggregated huntingtin. PLoS One **14**, e0213521, doi:10.1371/journal.pone.0213521 (2019).
11. Lin, L. *et al.* Transcriptome sequencing reveals aberrant alternative splicing in Huntington's disease. Hum Mol Genet **25**, 3454–3466, doi:10.1093/hmg/ddw187 (2016).
12. Elorza, A. *et al.* Huntington's disease-specific mis-splicing unveils key effector genes and altered splicing factors. Brain **144**, 2009–2023, doi:10.1093/brain/awab087 (2021).
13. Van Nostrand, E. L. *et al.* A large-scale binding and functional map of human RNA-binding proteins. Nature **583**, 711–719, doi:10.1038/s41586-020-2077-3 (2020).
14. Tabrizi, S. J. *et al.* Targeting Huntingtin Expression in Patients with Huntington's Disease. N Engl J Med **380**, 2307–2316, doi:10.1056/NEJMoa1900907 (2019).

15. Keller, C. G. *et al.* An orally available, brain penetrant, small molecule lowers huntingtin levels by enhancing pseudoexon inclusion. Nat Commun **13**, 1150, doi:10.1038/s41467-022-28653-6 (2022).
16. Bolger, A. M., Lohse, M. & Usadel, B. Trimmomatic: a flexible trimmer for Illumina sequence data. Bioinformatics **30**, 2114–2120, doi:10.1093/bioinformatics/btu170 (2014).
17. Dobin, A. *et al.* STAR: ultrafast universal RNA-seq aligner. Bioinformatics **29**, 15–21, doi:10.1093/bioinformatics/bts635 (2013).
18. Liao, Y., Smyth, G. K. & Shi, W. featureCounts: an efficient general purpose program for assigning sequence reads to genomic features. Bioinformatics **30**, 923–930, doi:10.1093/bioinformatics/btt656 (2014).
19. Shen, S. *et al.* rMATS: robust and flexible detection of differential alternative splicing from replicate RNA-Seq data. Proc Natl Acad Sci U S A **111**, E5593-5601, doi:10.1073/pnas.1419161111 (2014).

Figures

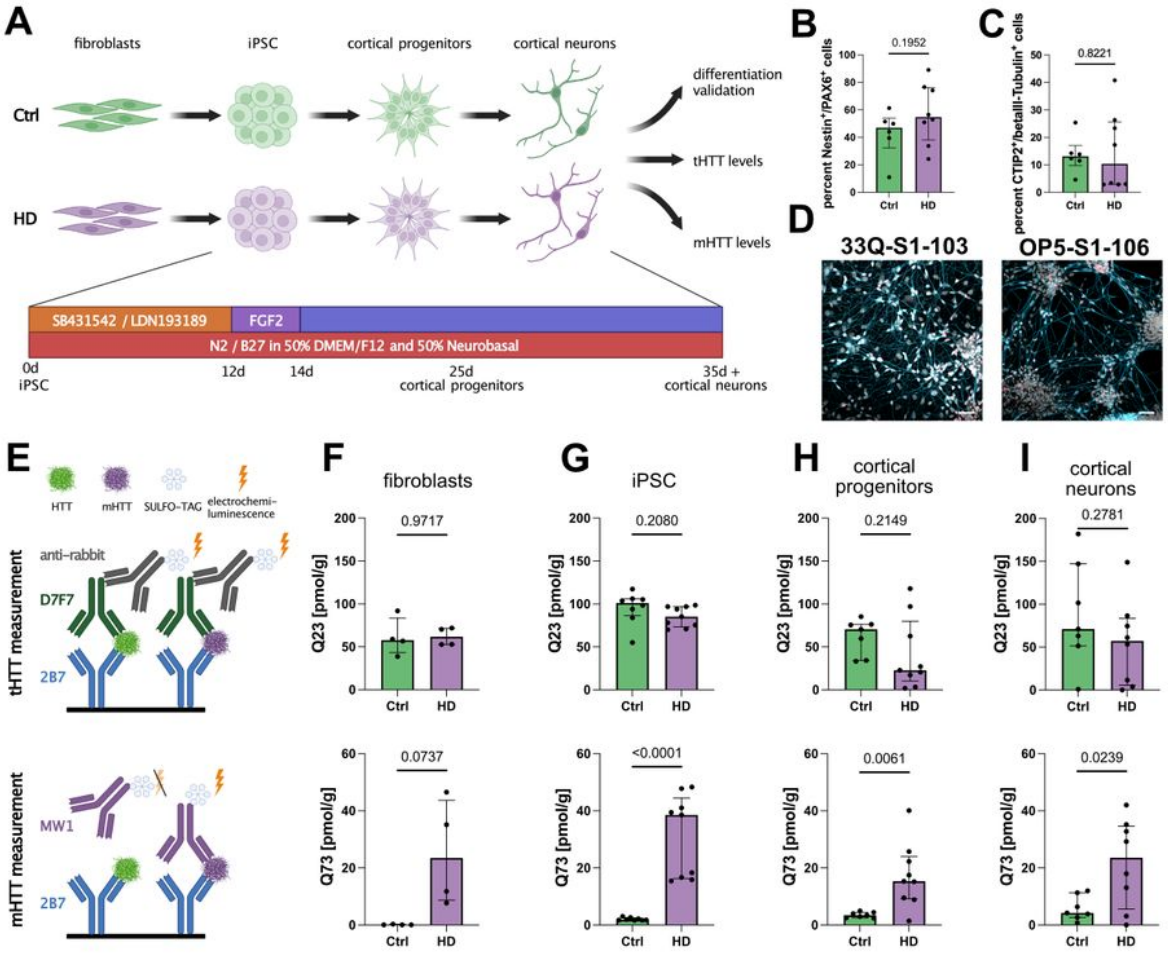

Figure 1

Mutant HTT is increased in HD patient-derived cells using a clinical grade assay

A Paradigm illustrating the HD patient-based disease model (fibroblasts, iPSC, cortical progenitors (25d old) and cortical neurons (35d old)) and readouts

B Bar plot depicting FACS quantification of NESTIN/PAX6 double-positive cells. Statistics: Welch’s test. Bars: median ± IQR.

C Bar plot illustrating FACS quantification of bIII-Tubulin/CTIP2 double-positive cells. Statistics: Welch’s test. Bars: median ± IQR.

D representative pictures of cortical neurons. Scale bar 50µm.

E Illustration depicting the MSD HTT quantification assay, where the added protein samples bind to 2B7 antibody, used for coating the plates. The SULFO-TAG coupled antibodies D7F7 and MW1 are added for quantification of total HTT and mutant HTT respectively.

F Bar plots quantifying total (tHTT, top) and mutant (mHTT, bottom) levels in fibroblasts (4 Ctrl lines, 4 HD lines). Statistics: tHTT: Welch's test (P value = 0.9717); mHTT: Welch's test (P value = 0.0737). Bars: median ± IQR.

G Bar plots quantifying total (tHTT, top) and mutant (mHTT, bottom) levels in iPSC (8 Ctrl lines, 9 HD lines). Statistics: tHTT: Welch's test (P value = 0.2080); mHTT: Mann-Whitney test (P value < 0.0001). Bars: median ± IQR.

H Bar plots quantifying total (tHTT, top) and mutant (mHTT, bottom) levels in cortical progenitors (7 Ctrl lines, 9 HD lines). Statistics: tHTT: Welch's test (P value = 0.2149); mHTT: Welch's test (P value = 0.0061). Bars: median ± IQR.

I Bar plots quantifying total (tHTT, top) and mutant (mHTT, bottom) levels in cortical neurons (7 Ctrl lines, 8 HD lines). Statistics: tHTT: Welch's test (P value = 0.2781); mHTT: Welch's test (P value = 0.0239). Bars: median ± IQR.

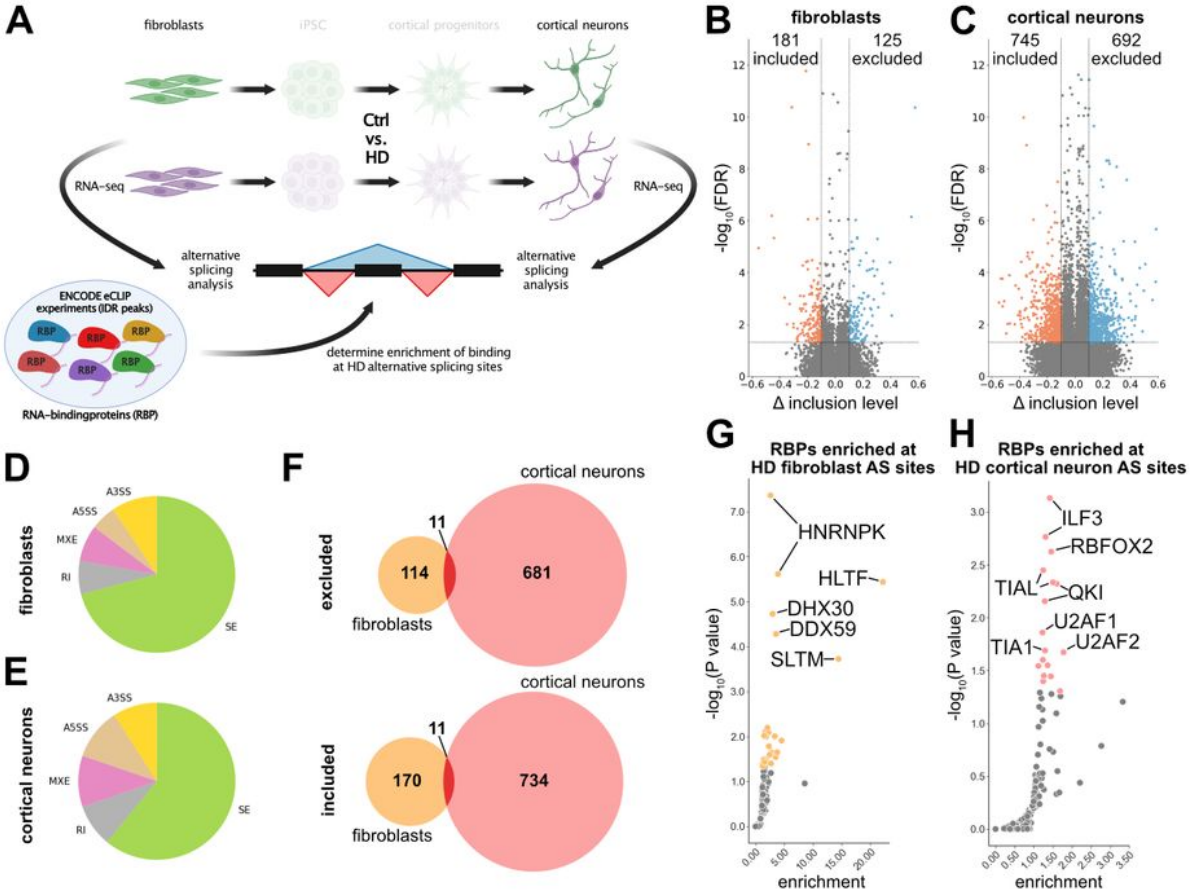

Figure 2

Aberrant alternative splicing is present in HD patients' fibroblasts and cortical neurons.

A Paradigm illustrating the analysis of fibroblasts and iPSC-derived cortical neurons (50d old) and integration of publicly available RNA-binding profile data (ENCODE eCLIP-seq) to determine degree and origin of alternative splicing in HD.

B Volcano plot showing inclusion levels difference (x) and significance (y) of alternative splicing events in Ctrl-DMSO vs HD-DMSO fibroblasts. Red: significantly included splicing events; blue: significantly excluded splicing events. Horizontal dashed line: FDR= 0.05; vertical dashed lines at -0.1 and 0.1.

C Volcano plot showing inclusion levels difference (x) and significance (y) of alternative splicing events in Ctrl-DMSO vs HD-DMSO iPSC-derived cortical neurons. Red: significantly included splicing events; blue: significantly excluded splicing events. Horizontal dashed line: FDR= 0.05; vertical dashed lines at -0.1 and 0.1.

D Pie chart of alternative splicing types in significant HD alternative splicing events in fibroblasts. Green: cassette exons (SE); yellow: alternative 3' splice site (A3SS); brown: alternative 5' splice site (A5SS); pink: mutually exclusive exons (MXE); gray: retained introns (RI)

E Pie chart of alternative splicing types in significant HD alternative splicing events in iPSC-derived cortical neurons. Green: cassette exons (SE); yellow: alternative 3' splice site (A3SS); brown: alternative 5' splice site (A5SS); pink: mutually exclusive exons (MXE); gray: retained introns (RI)

F Venn diagram showing overlap of significantly differentially spliced events in HD in fibroblasts and in neurons, respectively. Red depicts overlap between both cell types. Top graph: exon excluded in HD; bottom graph: exon included in HD.

G Scatter plot illustrating RNA-binding protein (RBP) RNA binding enrichment (x) and significance (y) at HD alternative splicing events in fibroblasts. Yellow colored dots depict RBPs with P value ≤ 0.05.

H Scatter plot illustrating RNA-binding protein (RBP) RNA binding enrichment (x) and significance (y) at HD alternative splicing events in iPSC cortical neurons. Salmon colored dots depict RBPs with P value ≤ 0.05.

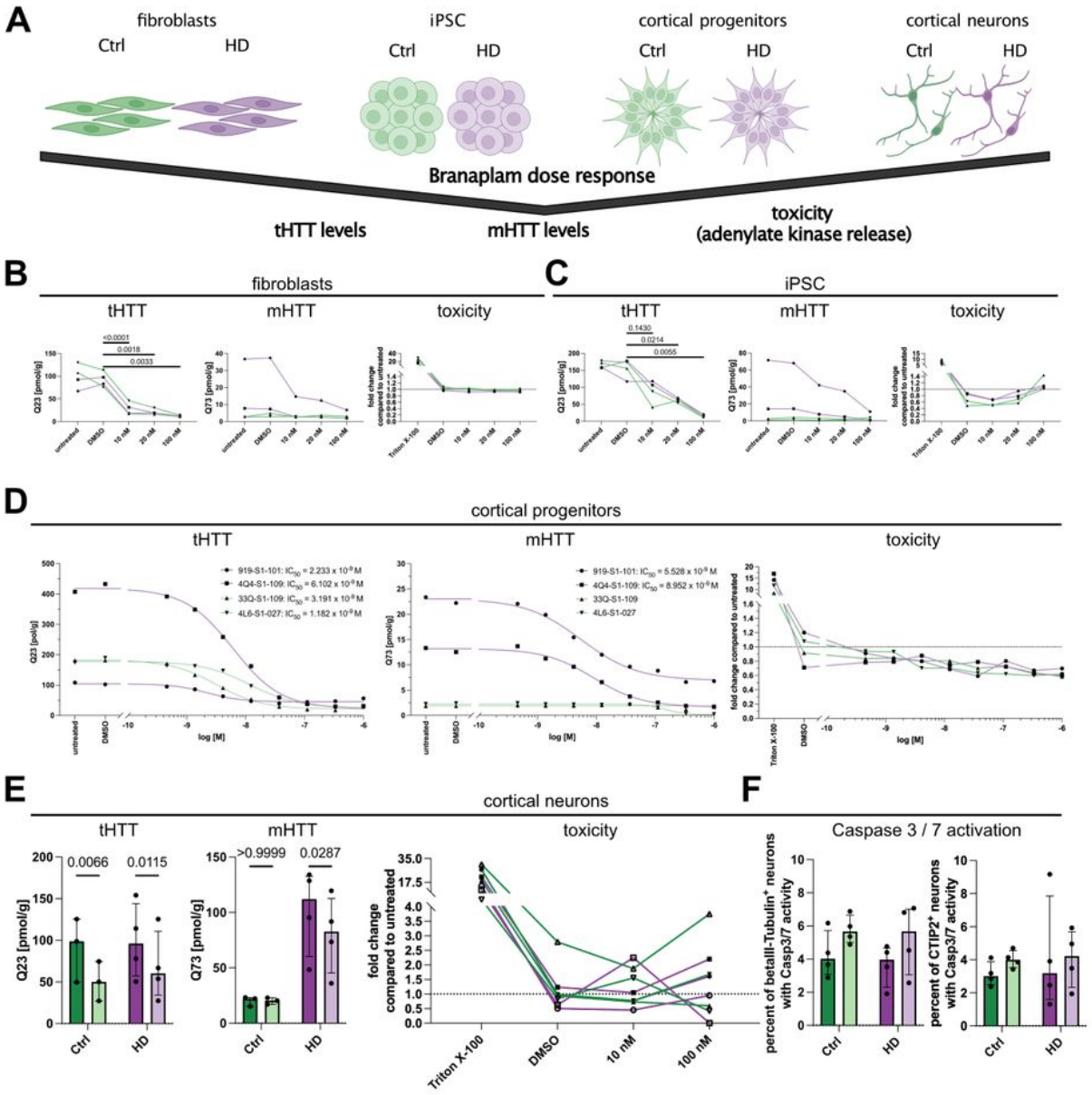

Figure 3

Branaplam reduces total and mutant HTT protein levels in a dose-dependent manner without inducing toxicity.

A Paradigm illustrating analyzed cell types (fibroblasts, iPSC, cortical progenitors (25d), cortical neurons (50d)) and parameters analyzed

B Line plots illustrating total HTT protein levels (tHTT), mutant HTT protein levels (mHTT) and toxicity measured by adenylate kinase release (toxicity, Triton X-100 as positive control) in fibroblasts with different Branaplam concentrations for 72h. Green: Ctrl samples (33Q and 4L6), purple: HD samples (919, 4Q4). Statistics: tHTT (n=4 (2 Ctrl + 2 HD)): one-way ANOVA with Geisser-Greenhouse correction (P = 0.0012); mHTT (n=2 (2 HD)): no statistics applied; toxicity (n=4 (2 Ctrl + 2 HD)) (Triton X-100 excluded): Friedman test (P = 0.0770).

C Line plots illustrating total HTT protein levels (tHTT), mutant HTT protein levels (mHTT) and toxicity measured by adenylate kinase release (toxicity, Triton X-100 as positive control) in iPSC with different Branaplam concentrations for 72h. Green: Ctrl samples (33Q-S1-109, 4L6-S1-027), purple: HD samples (919-S1-101, 4Q4-S1-109). Statistics: tHTT (n=4 (2 Ctrl + 2 HD)): one-way ANOVA with Geisser-Greenhouse correction (P = 0.0032); mHTT (n=2 (2 HD)): no statistics applied; toxicity (n=4 (2 Ctrl + 2 HD)) (Triton X-100 excluded): one-way ANOVA with Geisser-Greenhouse correction (P = 0.0455), no significant individual differences in multiple comparisons between groups.

D Line plots illustrating total HTT protein levels (tHTT), mutant HTT protein levels (mHTT) and toxicity measured by adenylate kinase release (toxicity, Triton X-100 as positive control) in cortical progenitors to calculate a dose response of Branaplam (DMSO, 0.43nM, 1.37nM, 4.1nM, 12.3nM, 37nM, 111.1nM, 333.3nM, 1000nM) for 72h. Green: Ctrl samples (33Q-S1-109, 4L6-S1-027), purple: HD samples (919-S1-101, 4Q4-S1-109). Statistics: tHTT IC_{50}: 919-S1-101 = 2.233 x 10^{-9} M; 4Q4-S1-109 = 6.102 x 10^{-9} M; 33Q-S1-109 = 3.191 x 10^{-9} M; 4L6-S1-027 = 1.182 x 10^{-9} M; mHTT: 919-S1-101 = 5.528 x 10^{-9} M; 4Q4-S1-109 = 8.952 x 10^{-9} M; 33Q-S1-109 = not calculated; 4L6-S1-027 = not calculated; toxicity (n=4 (2 Ctrl + 2 HD)) (Triton X-100 excluded): one-way ANOVA with Geisser-Greenhouse correction (P = 0.06).

E Bar plot illustrating total HTT protein levels (tHTT), mutant HTT protein levels (mHTT) (Ctrl n=3; HD n=4) and toxicity measured by adenylate kinase release (toxicity, Triton X-100 as positive control) in cortical neurons of (Ctrl n=4; HD n=4). tHTT and mHTT levels were measured with 10nM Branaplam for 72h. Statistics: tHTT: 2-way ANOVA (DMSO vs. Branaplam: P = 0.0009; Ctrl vs. HD: P = 0.6820; interaction: P = 0.3833); mHTT: 2-way ANOVA (DMSO vs. Branaplam: P = 0.0614; Ctrl vs. HD: P = 0.0223; interaction: P = 0.0615); toxicity (Triton X-100 excluded): Friedman test (P = 0.5306).

F Bar plot showing number of Casp3/7 positive betaIII-Tubulin+ and CTIP2+ cortical neurons after 72h 10nM Branaplam treatment (Ctrl n=4; HD n=4). Statistics: betaIII-Tubulin+: 2-way ANOVA (DMSO vs. Branaplam: P = 0.0782; Ctrl vs. HD: P = 0.4744; interaction: P = 0.9502); CTIP2+: 2-way ANOVA (DMSO vs. Branaplam: P = 0.7230; Ctrl vs. HD: P = 0.5779; interaction: P = 0.6348). Bars: median ± IQR.

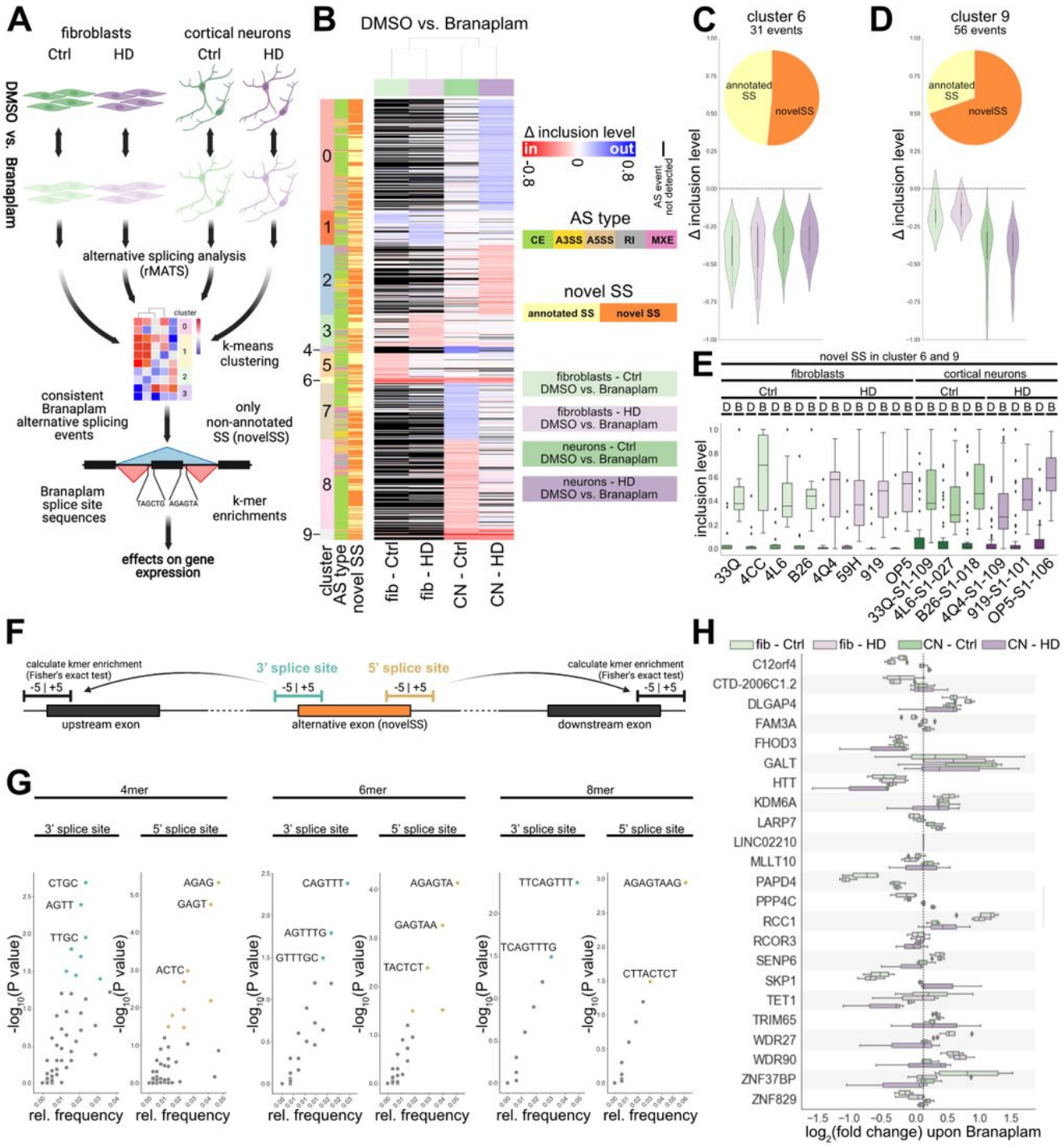

Figure 4

Branaplam promotes non-annotated exon inclusion at preferred sequences

A Paradigm illustrating analysis pipeline in the four analyzed conditions (light green: fibroblasts Ctrl DMSO vs. 10nM Branaplam (4 vs. 4); light purple: fibroblasts HD DMSO vs. 10nM Branaplam (4 vs. 4); green: cortical neurons (50d) Ctrl DMSO vs. 10nM Branaplam (3 vs. 3); purple: cortical neurons (50d) HD

DMSO vs. 10nM Branaplam (3 vs. 3)) . rMATS for alternative splicing detection and quantification, kmeans clustering to identify consistently changed alternative splicing events, kmer enrichment to investigate sequence preferences.

B Heatmap illustrating inclusion level differences of alternative splicing events significant (FDR $\leq$ 0.05; absolute inclusion level difference $\geq$ 0.1) in at least one of the four comparisons from included (red colors) to excluded (blue colors). Events not detected in an analysis are marked black. Y axis colors show alternative splicing cluster (0-9, determined by kmeans), alternative splicing type and novel splice sites.

C Violin plot and pie chart of alternative splicing events in cluster 6. Violin plot shows inclusion level difference in the four comparisons. Pie chart illustrates distribution of annotated (yellow) vs. non-annotated exons (novelSS, orange)).

D Violin plot and pie chart of alternative splicing events in cluster 9. Violin plot shows inclusion level difference in the four comparisons. Pie chart illustrates distribution of annotated vs. non-annotated exons (novelSS).

E Box plot showing inclusion values of alternative splicing events in cluster 6 and 9 that are non-annotated (novelSS) in individual samples. D: DMSO, B: Branaplam.

F Paradigm illustrating strategy to determine sequence preferences of Branaplam induced alternative splicing at the 5' exon (cyan) and 3' exon end (gold).

G Scatter plots of 4mer, 6mer and 8mer relative frequencies (x) and significance (y) at 3' splice site (respective left graph) and 5' splice site (respective right graph). Colored dots represent significant enrichments.

H Box plot illustrating gene expression changes ($\log_2$(RPKM Branaplam / RPKM DMSO)) of genes with alternative splicing events in cluster 6 and 9 that are non-annotated (novelSS) in all four comparisons. fib: fibroblasts, CN: cortical neurons.

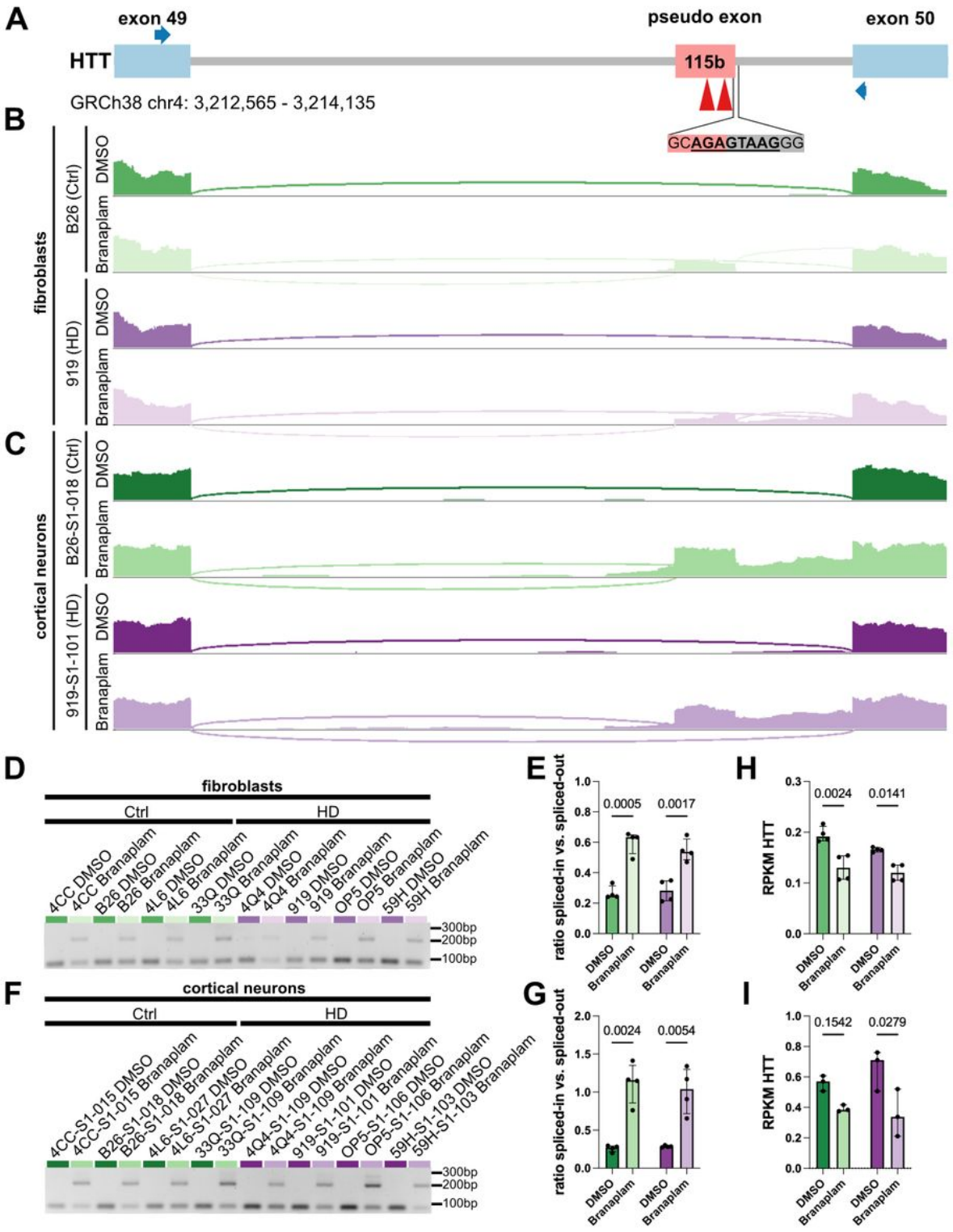

Figure 5

A frameshift inducing exon is inserted in HTT upon Branaplam treatment leading to reduction of HTT mRNA levels

A Illustration of locus with novel exon integrated in HTT transcript. Red arrowheads: in-frame STOP codons, blue arrows: primer locations for PCR validation.

B Sashimi plot illustrating read density and junction-spanning reads in Ctrl and HD fibroblasts with and without Branaplam.

C Sashimi plot illustrating read density and junction-spanning reads in Ctrl and HD cortical neurons with and without Branaplam.

D Agarose gel of PCR amplifying the HTT location of interest in fibroblasts with and without Branaplam. Lower band (88bp) represents regular transcript without exon inclusion, upper band (203bp) indicates integration of novel exon.

E Bar plot illustrating quantification of agarose gel. Depicted is the ratio of densitometric quantification of included vs. excluded HTT transcript in fibroblasts of Ctrl and HD with and without Branaplam treatment. Statistics: 2-way ANOVA (DMSO vs. Branaplam: $P < 0.0001$; Ctrl vs. HD: $P = 0.5954$; interaction: $P = 0.3139$). Bars: median ± IQR.

F Agarose gel of PCR amplifying the HTT location of interest in cortical neurons with and without Branaplam. Lower band (88bp) represents regular transcript without exon inclusion, upper band (203bp) indicates integration of novel exon.

G Bar plot illustrating quantification of agarose gel. Depicted is the ratio of densitometric quantification of included vs. excluded HTT transcript in cortical neurons of Ctrl and HD with and without Branaplam treatment. Statistics: 2-way ANOVA (DMSO vs. Branaplam: $P = 0.0003$; Ctrl vs. HD: $P = 0.7070$; interaction: $P = 0.5633$). Bars: median ± IQR.

H Bar plot illustrating HTT RPKM values in fibroblasts of Ctrl and HD with and without Branaplam treatment. Statistics: 2-way ANOVA (DMSO vs. Branaplam: $P = 0.0005$; Ctrl vs. HD: $P = 0.0777$; interaction: $P = 0.2603$). Bars: median ± IQR.

I Bar plot illustrating HTT RPKM values in cortical neurons of Ctrl and HD with and without Branaplam treatment. Statistics: 2-way ANOVA (DMSO vs. Branaplam: $P = 0.0101$; Ctrl vs. HD: $P = 0.6817$; interaction: $P = 0.2631$). Bars: median ± IQR.

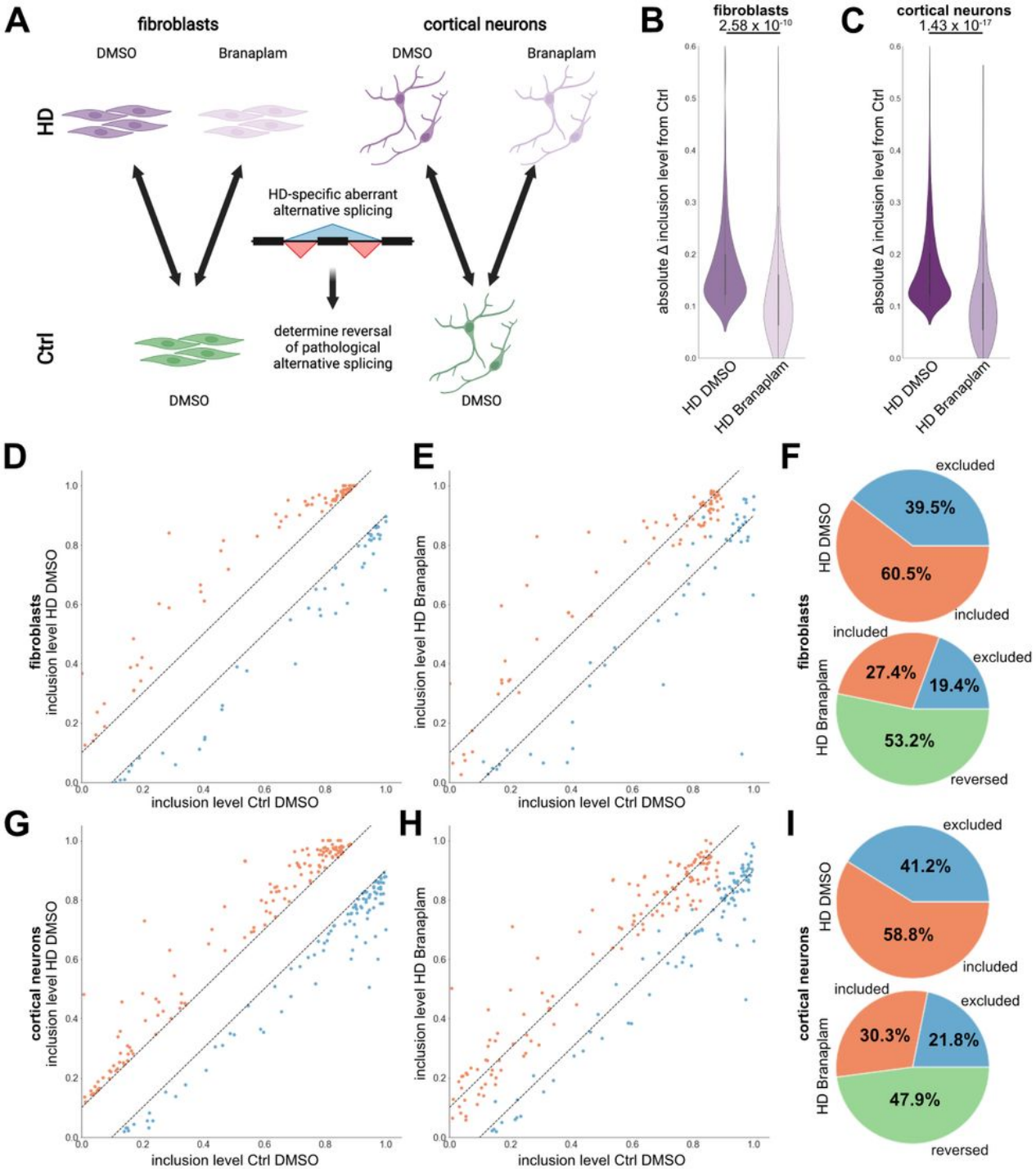

Figure 6

Branaplam improves alternative splicing pathology in HD fibroblasts and cortical neurons

A Paradigm illustrating samples used to determine improvements in alternative splicing pathology.

B Violin plot showing absolute inclusion level differences (Ctrl DMSO - HD DMSO and Ctrl DMSO - HD Branaplam) of HD alternative splicing events detected in all fibroblast samples. Significance is calculated with Wilcoxon ranksum test using scipy.stats..

C Violin plot showing absolute inclusion level differences (Ctrl DMSO - HD DMSO and Ctrl DMSO - HD Branaplam) of HD alternative splicing events detected in all cortical neuron samples. Significance is calculated with Wilcoxon ranksum test using scipy.stats..

D Scatter plot illustrating inclusion levels of HD alternative splicing events detected in all fibroblast samples in Ctrl DMSO (x) and HD DMSO (y). Dashed lines mark corridor of absolute inclusion level difference < 0.1. Red: events included in HD fibroblasts, blue: events excluded in HD fibroblasts.

E Scatter plot illustrating inclusion levels of HD alternative splicing events detected in all fibroblast samples in Ctrl DMSO (x) and HD Branaplam (y). Dashed lines mark corridor of absolute inclusion level difference < 0.1. Red: events included in HD fibroblasts, blue: events excluded in HD fibroblasts.

F Pie charts quantifying percentage of number of events changed in HD fibroblasts that are excluded, included or rescued (within absolute inclusion level difference corridor < 0.1) in HD DMSO (top chart) and HD Branaplam (bottom chart).

G Scatter plot illustrating inclusion levels of HD alternative splicing events detected in all cortical neurons samples in Ctrl DMSO (x) and HD DMSO (y). Dashed lines mark corridor of absolute inclusion level difference < 0.1. Red: events included in HD cortical neurons, blue: events excluded in HD cortical neurons.

H Scatter plot illustrating inclusion levels of HD alternative splicing events detected in all cortical neurons samples in Ctrl DMSO (x) and HD Branaplam (y). Dashed lines mark corridor of absolute inclusion level difference < 0.1. Red: events included in HD cortical neurons, blue: events excluded in HD cortical neurons.

I Pie charts quantifying percentage of number of events changed in HD cortical neurons that are excluded, included or rescued (within absolute inclusion level difference corridor < 0.1) in HD DMSO (top chart) and HD Branaplam (bottom chart).

Supplementary Files

This is a list of supplementary files associated with this preprint. Click to download.

- Files.zip
- extendeddatafigure1.jpg

- extendeddatafigure2.jpg
- extendeddatafigure3.jpg